Modeling of the Catalytic Removal of CO and NO in Dry Combustion Gases

C. Treviño
UMDI, Facultad de Ciencias, Universidad Nacional Autónoma de México, Sisal, Yucatán, México

J. C. Prince
Instituto Tecnológico de Veracruz, Dept. de Metal Mecánica, Veracruz, México

DOI 10.1002/aic.11988
Published online August 20, 2009 in Wiley InterScience (www.interscience.wiley.com).

Catalytic removal of pollutants in dry combustion gases in a planar stagnation-point flow over a platinum foil is studied using both numerical and analytical tools. The governing equations have been numerically integrated with the Newton technique, and the response curve has been obtained as functions of temperature and the mixture concentrations. Using the appropriate stoichiometry, the additional oxygen needed to reduce the NO and to achieve complete oxidation of CO has been obtained. The asymptotic analysis leads to an algebraic equation for the surface coverage of empty sites as a function of two nondimensional parameters: the mass transfer number, relating the residence time to the chemical time (sort of Damköhler number), and a parameter, which relates the desorption rate to the adsorption rate of carbon monoxide and depends strongly on temperature. Critical conditions of ignition (light-off) and extinction are identified and closed form solutions are obtained for these phenomena. © 2009 American Institute of Chemical Engineers *AIChE J,* 56: 801–809, 2010
Keywords: catalysis, computational chemistry (at solid surfaces), reactor analysis, simulation, process, surface chemistry/physics

Introduction

Theoretical and experimental studies of catalytic combustion and ignition have been carried out in the last decades for both practical and fundamental reasons. The removal of polluting agents, such as NO_x and CO, of combustion gases by catalytic means is one of the main subjects of interest in the environmental studies. A catalytic converter is a device used to reduce the toxicity of emissions from an internal combustion engine. This after-treatment device consists of a monolith encased in a metal designed to distribute the exhaust flow evenly.[1–3] The active catalytic material used to convert the polluting emissions is distributed over a large surface area to promote chemical reactions, between the gas phase and the active catalytic surface, that convert pollutants into harmless gases and water. Most modern cars are equipped with Three-Way Catalytic (TWC) converters. ''Three-way'' refers to the three regulated emissions that helps to reduce carbon monoxide, unburnt hydrocarbons, and nitrogen oxide gases, provided that the engine operates at a stoichiometric fuel–air mixture. The most common employed metals as catalytic surfaces are platinum, rhodium, and palladium and sometimes other catalysts such as the rare earth ceria.[4–7]

The fundamentals of heterogeneous catalysis have been described elsewhere,[1–17] where several surface reaction mechanisms for Pt, Rh, and Pd catalyst are proposed for the oxidation of CO and reduction of NO_x. The ignition process is characterized by an abrupt transition from a kinetically controlled system to one controlled by mass transport and depends mainly on the adsorption–desorption reaction steps. Experimental studies have also shown that exhaust gases coming at lower temperature and from an engine running slightly below the stoichiometric point are beneficial for

Correspondence concerning this article should be addressed to C. Treviño at ctrev@servidor.unam.mx

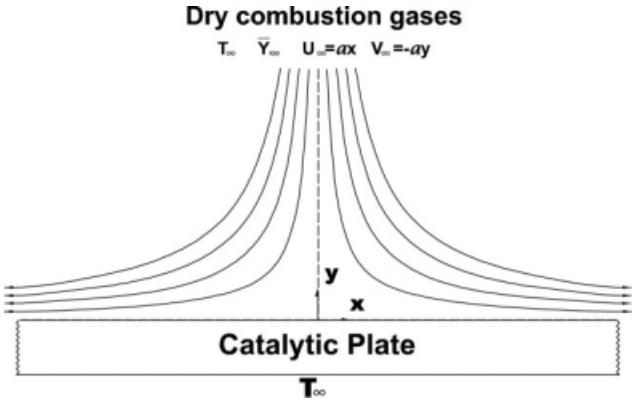

Figure 1. Stagnation-point flow configuration used in this work.

NO_x control but in detrimental to CO emissions. On the other hand, CO oxidizes rapidly at high temperatures in the presence of oxygen, at the expense of NO_x reduction reaction.

Catalytic converter models have been appearing in the literature at the same time with the development of new catalytic converter technologies. In the numerical studies, heterogeneous reactions mechanisms are used to describe surface reactions on catalytic plates, where the chemical species are absorbed, reacting on the plate of the catalyst, followed by a desorption step. Catalytic ignition has been studied by either using elementary chemistry or by large activation energy asymptotic analyses applying a one-step overall reaction mechanism.[5–18] Reduced reaction mechanisms are also used, with a limited number of phenomenological reactions that contain only initial reactants and final products instead of elementary reactions on the catalyst active sites. However, a reliable, quantitative reaction mechanism capable of capturing experimentally observed features is not available. Necessity exists to obtain reduced kinetic schemes for the catalytic combustion that help to construct a bridge between the full numerical works and the theories developed using an overall one-step reaction for the surface kinetics. The objective of this work is to extend the analysis[14] obtained for the catalytic combustion of dry carbon monoxide, to the catalytic removal of CO + NO in dry hot combustion gases over a platinum catalyst using the stagnation-point flow configuration, where inlet experimental data will be used for the simulation and analysis.

Problem Formulation

A two-dimensional flow problem, which can be reduced to a one dimensional problem using a self-similar formulation, is used in this work to reduce the flow complexity and to extract the main features of the process. The physical model of the catalytic pollutant remover under study is shown in Figure 1, where the stagnation-point flow geometry is used. A mixture of dry combustion gases including CO, NO, and excess O_2 described by the mass concentrations $\overline{Y}_{CO_\infty}$, $\overline{Y}_{O_{2\infty}}$, and $\overline{Y}_{NO_\infty}$ and temperature T_∞, flows perpendicular towards a catalytic plate, with a velocity gradient a. The surface of the plate is kept at a uniform temperature equal to that of the combustion gases, T_∞. The boundary layer governing equations,[19,20] assuming a chemically frozen gas-phase are given by

$$\frac{\partial(\rho u)}{\partial x}+\frac{\partial(\rho v)}{\partial y}=0, \tag{1}$$

$$\rho u\frac{\partial u}{\partial x}+\rho v\frac{\partial u}{\partial y}=\frac{\partial}{\partial y}\left(\mu\frac{\partial u}{\partial y}\right)+\rho_\infty a^2 x, \tag{2}$$

$$\rho u\frac{\partial \overline{Y}_i}{\partial x}+\rho v\frac{\partial \overline{Y}_i}{\partial y}=\frac{\partial}{\partial y}\left(\rho D_i\frac{\partial \overline{Y}_i}{\partial y}\right), \tag{3}$$

where u and v are the longitudinal and transverse components of velocity, respectively. ρ and μ are the density and viscosity of the gas-phase mixture. D_i corresponds to the mass diffusion coefficient of species i in the mixture. The associated boundary conditions at the plate surface are the following

$$u=v=\frac{\partial \overline{Y}_i}{\partial y}-\frac{\omega_i W_i}{\rho D_i}=0 \quad \text{at} \quad y=0 \tag{4}$$

$$u-ax=\overline{Y}_i-\overline{Y}_{i\infty}=0, \quad \text{for} \quad y\to\infty. \tag{5}$$

Here, W_i is the molecular weight of species i, and ω_i is the surface reaction rate given in units of mol of species i consumed by unit time unit surface of the plate. In the above equations, it has been assumed that the heat release from the catalytic surface reactions are negligible small to change the gas temperature due to the small pollutant concentrations.

The nondimensional form of the governing Eq. 1–5 is given by

$$\frac{d^3 f}{d\eta^3}+f\frac{d^2 f}{d\eta^2}+1-\left(\frac{df}{d\eta}\right)^2=0, \tag{6}$$

$$\frac{d^2 Y_i}{d\eta^2}+fSc_i\frac{dY_i}{d\eta}=0, \tag{7}$$

where f is the nondimensional stream function, $f=\psi/(x\sqrt{\rho_\infty\mu_\infty a})$, Y_i is the reduced species concentration $Y_i=\overline{Y}/\overline{Y}_{i\infty}$, and η is a normalized nondimensional coordinate scaled with the flow characteristic length or boundary layer thickness $l_f=\sqrt{\mu_\infty/(\rho_\infty a)}$, $\eta=y/l_f$. Sc_i are the Schmidt numbers of the species, $Sc_i=\mu_\infty/\rho_\infty D_i$. The resulting nondimensional boundary conditions are then given by

$$f=\frac{df}{d\eta}=\frac{dY_i}{d\eta}-G_i=0 \quad \text{at} \quad \eta=0, \tag{8}$$

$$\frac{df}{d\eta}-1=Y_i-1=0 \quad \text{at} \quad \eta\to\infty, \tag{9}$$

where

$$G_i=\frac{\omega_i W_i Sc_i}{\mu_\infty \overline{Y}_{i\infty}}l_f, \tag{10}$$

All the information about the characteristic flow time, given by the velocity gradient a, is contained in the surface source term functions G_i, which are a sort of Damköhler numbers.

Table 1. Heterogeneous Reaction Model and the Kinetic Parameters

NO	Elementary Reaction	S	A	E
1a	$CO + * \rightarrow CO*$	0.84		
1d	$CO* \rightarrow CO + *$		10^{13}	125.5
2a	$O_2 + 2* \rightarrow 2O*$	$0.07\frac{300}{T}$		
2d	$2O* \rightarrow O_2 + 2*$		3.7×10^{21}	213.2
3	$CO* + O* \rightarrow CO_2^* + *$		3.7×10^{21}	105
4a	$CO_2 + * \rightarrow CO_2^*$	0.05		
4d	$CO_2^* \rightarrow CO_2 + *$		10^{13}	20.5
5a	$NO + * \rightarrow NO*$	0.85		
5d	$NO* \rightarrow NO + *$		3.04×10^{10}	83.2
6d	$2N* \rightarrow N_2 + 2*$		4.08×10^{8}	56.6
7	$NO* + * \rightarrow N* + O*$		2.19×10^{5}	45.8

k, [$m^3\ mol^{-1}s^{-1}$]; A, [s^{-1}]; E [kJ, mol^{-1}]; S, [−].

The theory developed here can be used with any other flow configuration by changing the proper characteristic length, l_f. The surface chemical reaction terms ω_i are to be obtained by using the corresponding surface chemistry model.

Heterogeneous Reaction Model

The heterogeneous model used in this work is a detailed set of surface reactions which includes the CO, NO, and O_2 chemistry, represented by the reaction mechanism shown in Table 1.[14,21] The reactions labels ending with a, d, and r represent adsorption, desorption, and surface reaction processes, respectively. The symbol * denotes a free site on the catalyst, which is in this case platinum, and the species with superindex * denotes an adsorbed species on the surface of the catalyst. Reactions 3 and 7 are surface reactions that are assumed to be of the Langmuir–Hinshelwood type. It must be noticed that the production of O* by the adsorption of the NO is used for the oxidation of the CO*. Because of the fact that, in general, the concentration of NO in combustion gases are very small compared with that of carbon monoxide, this O* is not sufficient for the complete oxidation of CO*. Therefore, additional oxygen is needed, as reported in experimental research. The adsorption kinetics is controlled by a sticking probability, S_i or accommodation coefficient, which represents the portion of the collisions of i species with the surface that successfully leads to adsorption. The rate of collisions are computed using the classical kinetic theory. On the other hand, the desorption kinetics is well-represented by an Arrhenius law, with a high activation energy for the surface species CO* and O*. The adsorbed species concentrations are represented by the surface coverage θ_i defined by the number of sites occupied by surface species to the total number of available sites.

The adsorption reaction rates are given by

$$k_{ra} = \frac{S_i p \overline{Y}_{iw} W}{\Gamma W_i^{3/2} \sqrt{2\pi RT}}, \tag{11}$$

where the species i correspond to that described by reaction r. Here, Γ is the molar concentration of the surface in mol/cm^2 of active sites and corresponds to the density of active sites in the surface divided by the Avogadro number. In this work a value of $\Gamma = 1.6603 \times 10^{-9}$ mol/cm^2[28] has been assumed for simplicity. Any other value of Γ and catalyst type can be used in the analysis what follows, by using the appropriate rates. R is the universal constant of the gases, p is the pressure, W is the molecular weight of the mixture, and $\overline{Y}_{iw}$ is the concentration of species i close to the catalytic surface and are to be obtained after solving the governing equations. The desorption reaction rates are given by

$$k_{rd} = \Gamma^{n_r} A_{rd} \quad \exp\left(\frac{-\mathrm{E_{rd}}}{\mathrm{RT}}\right), \tag{12}$$

where A_{rd}, E_{rd}, and n_r are the frequency factor, the activation energy, and the reaction order of the desorption reaction r, respectively. All reaction rates are given in s^{-1} units. For the adsorbed species, the steady-state conservation equations are given by

$$\frac{d\theta_{CO}}{dt} = 0 = k_{1a\infty} Y_{CO\,w} \theta_* - k_{1d}\theta_{CO} - k_3 \theta_{CO}\,\theta_O \tag{13}$$

$$\frac{d\theta_O}{dt} = 0 = 2k_{2a\infty} Y_{O_2 w} \theta_*^2 - 2k_{2d}\theta_O^2 - k_3 \theta_{CO}\,\theta_O + k_7 \theta_{NO}\,\theta_* \tag{14}$$

$$\frac{d\theta_{CO_2}}{dt} = 0 = k_3 \theta_{CO}\,\theta_O - k_{4d}\theta_{CO_2} + k_{4a\infty} Y_{CO_2 w} \theta_* \tag{15}$$

$$\frac{d\theta_{NO}}{dt} = 0 = k_{5a\infty} Y_{NO\,w} \theta_* - k_{5d}\theta_{NO} - k_7 \theta_{NO}\,\theta_* \tag{16}$$

$$\frac{d\theta_N}{dt} = 0 = -2k_{6d}\theta_N^2 + k_7 \theta_{NO}\,\theta_* \tag{17}$$

$$\theta_* = 1 - \theta_{CO} - \theta_O - \theta_{CO_2} - \theta_{NO} - \theta_N. \tag{18}$$

Here θ_* denotes the surface coverage of empty or vacant sites. The adsorption rates described with subindex ∞ denotes the rates using the species concentrations with their values of the combustion gases far from the catalytic plate. The chemical reaction terms ω_i are using the present chemistry model

$$\omega_{CO} = \Gamma k_3 \theta_{CO}\,\theta_O, \quad \omega_{NO} = \Gamma k_7 \theta_{NO}\,\theta_*, \quad 2\omega_{O_2} = \Gamma k_3 \theta_{CO}\,\theta_O - \Gamma k_7 \theta_{NO}\,\theta_*. \tag{19}$$

From these relationships, it can be obtained the following

$$\omega_{CO} = 2\omega_{O_2} + \omega_{NO}, \tag{20}$$

which gives the overall reaction

$$CO + \alpha NO + \frac{1-\alpha}{2} O_2 \rightarrow CO_2 + \frac{\alpha}{2} N_2, \tag{21}$$

where $\alpha = (W_{CO}/W_{NO})(Y_{NO_\infty}/Y_{CO_\infty})$. From the steady-state relationships 13–18, it is preferable to use the adsorption and desorption rates instead of those involving reactions between adsorbed species, due to the high uncertainty on the rate constants. In this case, relationships (19) reduce to

$$\omega_{CO} = \Gamma k_{1a\infty} Y_{COw} \theta_* - \Gamma k_{1d} \theta_{CO} \quad (22)$$

$$\omega_{NO} = \Gamma k_{5a\infty} Y_{NOw} \theta_* - \Gamma k_{5d} \theta_{NO} \quad (23)$$

$$\omega_{O_2} = \Gamma k_{2a\infty} Y_{O_2 w} \theta_*^2 - \Gamma k_{2d} \theta_O^2 \quad (24)$$

Analytical Solution of the Governing Equations

The solution of the universal nonlinear momentum Eq. 6, with the corresponding boundary conditions (8) and (9) is straight forward using numerical methods and can be found elsewhere.[19] Once the nondimensional stream function $f(\eta)$ is obtained numerically, the solution of the mass conservation Eq. 7 are then given by

$$Y_i = Y_{iw} + G_i \int_0^{\eta} \exp\left\{-Sc_i \int_0^{\eta_1} f(\eta_2) d\eta_2\right\} d\eta_1. \quad (25)$$

Using the boundary conditions (8) and (9), the resulting normalized concentration at the catalytic surface is then

$$Y_{iw} = 1 - G_i \int_0^{\infty} \exp\left\{-Sc_i \int_0^{\eta} f(\eta_1) d\eta_1\right\} d\eta. \quad (26)$$

It is an excellent approximation for all gaseous species considered in this work to assume Schmidt numbers of unity. For a Schmidt number of unity,[19]

$$\int_0^{\infty} \exp\left\{-\int_0^{\eta} f(\eta) d\eta\right\} = I \simeq 4.4643. \quad (27)$$

and therefore

$$Y_{iw} = 1 - IG_i \quad (28)$$

The main target in this work is to obtain Y_{COw} and Y_{NOw}, which depends mainly on the temperature of the gases. Because the activation energy of the desorption reaction of oxygen 2d is extremely high, the desorption rate is negligible small compared with the adsorption reaction, for temperatures below 900 K and therefore, the consumption rate of oxygen is dictated only by its adsorption rate, $\omega_{O_2} = \Gamma k_{2a\infty} Y_{O_{2w}} \theta_*^2$. In this case, from Eqs. 24 and 28, the reduced concentration of oxygen close to the surface, can be obtained as a function of the surface coverage of empty sites as

$$Y_{O_2 w} = \frac{1}{1 + B_{O_2} \theta^{*2}}, \quad (29)$$

where B_{O_2} is the mass transfer number defined by

$$B_{O_2} = \frac{\Gamma k_{2a\infty} W_{O_2} l_f I}{\mu_\infty \overline{Y}_{O_2 \infty}}. \quad (30)$$

Large mass transfer numbers compared with unity are needed to remove the pollutants in an efficient way. Eq. 29 indicates that more oxygen is consumed as the surface coverage of empty sites increases. The consumption rate of oxygen is then

$$\omega_{O_2} = \frac{\Gamma k_{2a\infty} \theta_*^2}{1 + B_{O_2} \theta_*^2} = \overline{\omega_{O_2}} \frac{B_{O_2} \theta^{*2}}{1 + B_{O_2} \theta^{*2}}, \quad (31)$$

where

$$\overline{\omega_{O_2}} = \frac{\mu_\infty \overline{Y}_{O_2 \infty}}{W_{O_2} l_f I} \quad (32)$$

is the maximum possible consumption rate of molecular oxygen. Knowing that the consumption rate of carbon monoxide is at least twice the consumption rate of oxygen (for the cases where the NO concentration is negligible small compared with that of CO), Eq. 13 takes the form

$$1 \simeq \frac{\beta \theta_{CO}}{Y_{COw} \theta_*} + \frac{2 k_{2a\infty}}{k_{1a\infty}} \frac{Y_{O_2 w}}{Y_{COw}} \theta_*, \quad (33)$$

where $\beta = k_{1d}/k_{1a\infty}$ depends strongly on temperature. In general, the second term on the right hand side is much lower than unity; therefore, the first term on the right hand side must be close to unity, indicating that the reaction rate is much more lower than the adsorption and desorption reactions for the carbon monoxide, that is, the adsorption–desorption of carbon monoxide is assumed to be in partial equilibrium.

For relatively low temperatures, the overall reaction rates are very small, several orders of magnitude lower than the adsorption rates of CO and NO. The surface coverages at this low temperature can be then obtained from the two species Langmuir isotherm

$$\theta_* = \beta \theta_{CO} \quad (34)$$

$$\theta_{NO} = \frac{\beta}{\beta_5} \theta_{CO}, \quad (35)$$

where $\beta_5 = k_{5d}/k_{5a\infty}$. At low temperatures, typical values of β and β_5 are 10^{-17} and 10^{-10}, respectively. Therefore, at low temperatures, $\theta_{CO} \simeq 1$ with $\theta_* \simeq \beta$ and $\theta_{NO} \simeq \beta/\beta_5$. The catalyst is poisoned by adsorbed carbon monoxide. As the temperature increases, the rate of the desorption reactions increase significantly, thus freeing active sites on the catalytic surface and producing an increase of the surface coverage of empty sites and therefore increasing the reaction rate. The surface coverage of CO and * must be considered, while the rest of the coverages of the adsorbed species are extremely small compared with unity at all considered temperatures and thus can be neglected in the overall balance Eq. 18. An excellent assumption is

$$\theta_{CO} \simeq 1 - \theta_*. \quad (36)$$

Using this approximation in Eq. 33, it can be obtained the reduced concentration of carbon monoxide close to the catalytic wall as a function of the coverage of empty sites

$$Y_{COw} = \frac{\beta(1 - \theta_*)}{\theta_*}. \quad (37)$$

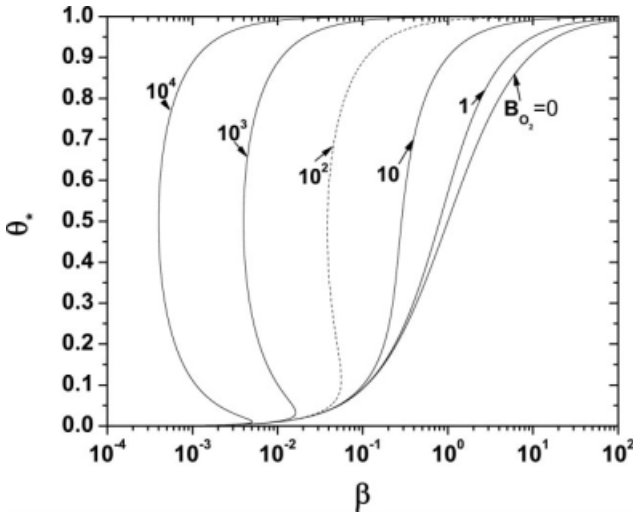

Figure 2. Solution of the cubic Eq. 38.

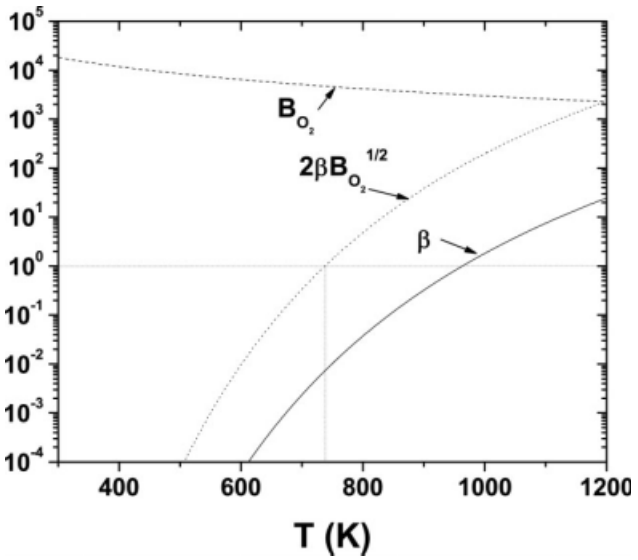

Figure 3. Parameters β and B_{O_2} as functions of temperature.

Parameter $2\beta B_{O2}^{1/2}$ is also plotted which has to be unity at ignition.

As the Schmidt numbers for CO and O_2 were assumed to be unity and from the overall stoichiometry given by the global reaction (21), close to the wall the reduced concentrations for both species are the same, $Y_{COw} \approx Y_{O_2 w}$, and using Eq. 29, an algebraic cubic equation for θ_* is obtained as a function of two nondimensional parameters: β and B_{O_2},

$$\beta B_{O_2}\theta_*^3 - \beta B_{O_2}\theta_*^2 + (1+\beta)\theta_* - \beta = 0. \tag{38}$$

Figure 2 shows the solution of (38) for different values of B_{O_2}. For values of $B_{O_2} < 27.01$, a single-valued function is obtained, whereas for larger mass transfer numbers, three different values of the surface coverage are obtained for a given value of the parameter β, in a narrow window. Figure 3 shows the value of parameter β as a function of temperature, showing the strong dependence due to the relatively high activation energy of the desorption reaction of carbon monoxide. For large values of the mass transfer number compared with unity, which is required to achieve high removal efficiency, Eq. 38 shows a typical S-shaped curve with three different solution branches. A weakly reactive branch with $\theta_* \sim \beta \sim B_{O_2}^{-1/2} \to 0$ and a strongly reactive branch with $\theta_* \sim 1$. The middle reaction branch with negative slope $d\theta_*/d_\beta$ is unstable. For the weakly reactive branch, Eq. 38 can be simplified using the fact that $\beta \ll 1$ and $\theta_*^3 \ll \theta_*^2$, resulting

$$\beta B_{O_2}\theta_*^2 - \theta_* + \beta \simeq 0, \tag{39}$$

with the solution

Table 2. Typical Dry Exhaust Gas Mass Concentrations

Components	Mass Fraction
CO	0.014
NO	0.0013
O_2	Varied
CO_2	0.17904
N_2	Rest

$$\theta_* = \frac{1}{2\beta B_{O_2}} \pm \frac{\sqrt{1 - 4\beta^2 B_{O_2}}}{2\beta B_{O_2}}. \tag{40}$$

For values of $\beta > \beta_I = (4B_{O_2})^{-1/2}$, there is no a real solution, indicating clearly the existence of the light-off or ignition condition, which can be used to determine the ignition temperature, T_I as

$$T_I = \frac{E_{1d}}{R \ln\left[2A_{1d}B_{O_2}^{1/2}/k_{1a\infty}\right]}. \tag{41}$$

The light-off temperature therefore depends only on the adsorption rates of CO and O_2 (through B_{O_2}), and the desorption rate of CO. On the other hand, for the strongly reactive branch, with θ_* of order unity, the resulting quadratic equation takes the form

$$\beta B_{O_2}\theta_*^2 - \beta B_{O_2}\theta_* + 1 = 0, \tag{42}$$

with the solution

$$\theta_* = \frac{1}{2} \pm \sqrt{\frac{1}{4} - \frac{1}{\beta B_{O_2}}}, \tag{43}$$

indicating the existence of the extinction condition for values of $\beta < \beta_E = 4/B_{O_2}$. The extinction temperature, T_E is then

$$T_E = \frac{E_{1d}}{R \ln\left[A_{1d}B_{O_2}/4k_{1a\infty}\right]}. \tag{44}$$

Numerical Results and Discussion

The governing equations represented by the algebraic set of nonlinear Eqs. 13–18 and 28 are solved numerically using

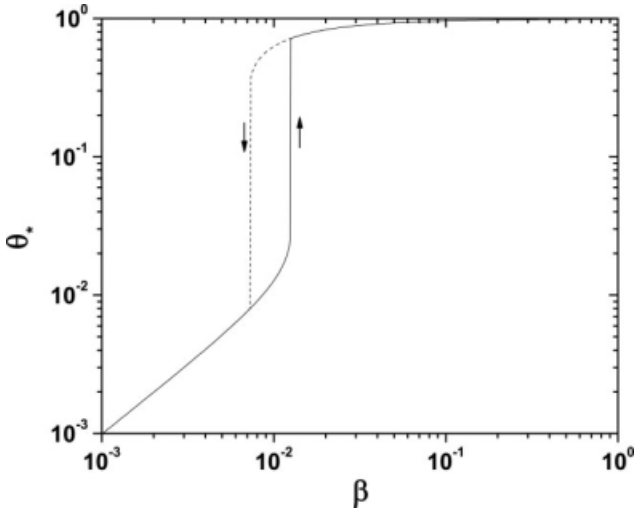

Figure 4. Surface coverage of empty sites as a function of parameter β.

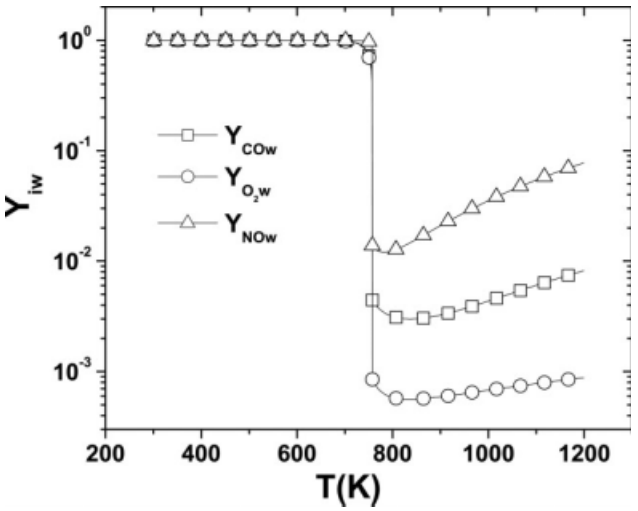

Figure 6. Reduced concentration of gaseous species close to the catalytic wall as functions of temperature.

the Newton technique. The resulting computational code was written in Fortran and the simulation was carried out in a workstation in a Linux environment. Numerical simulations were carried out for the reduction of NO and oxidation of CO in the absence and presence of O_2. The reduced mass concentrations of the chemical species close to the surface represented by Y_{iw} and the surface coverages θ_i are strongly influenced by the amount of O_2 present in the combustion gases and the gas (and catalyst) temperature. For a given surface temperature, the corresponding values of θ_i and Y_{iw} are computed. The temperature is then increased from 300 K to 1200 K and then decreased down to 300 K, to obtain the hysteresis response of the process. For this work, the assumed combustion gases concentrations (dry and without any unburnt fuel) composed by CO, NO, O_2, CO_2, and N_2 is given in Table 2.[21]

The amount of O_2 required is varied to achieve maximum CO and NO removal and is mainly dictated by the overall stoichiometry given by reaction (21). In this case, $\alpha = 0.0926$ and $\overline{Y}_{NO\infty} = 0.00591$. For simplicity, only the case of a velocity gradient of $a = 1\ s^{-1}$ is considered. Any other value only changes the value of the characteristic length l_f and is reflected on the mass transfer number B_{O_2} which is proportional to $a^{-1/2}$. Once the ignition temperature for the case $a = 1$ is obtained, T_{I1}, the ignition temperature at any other value of the flow velocity gradient a can be estimated after neglecting the weak temperature dependence on the adsorption rates, resulting

$$T_I = \frac{T_{I1}}{1 - \frac{RT_{I1}\ln(a)}{E_{1d}}}. \tag{45}$$

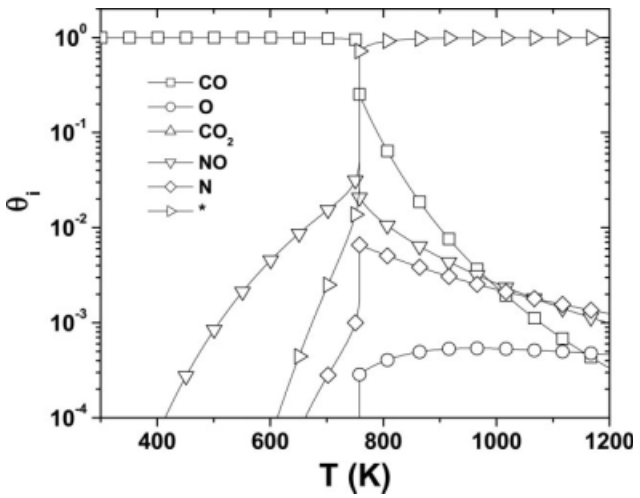

Figure 5. Surface coverage of adsorbed species as functions of the temperature, obtained as the temperature increases.

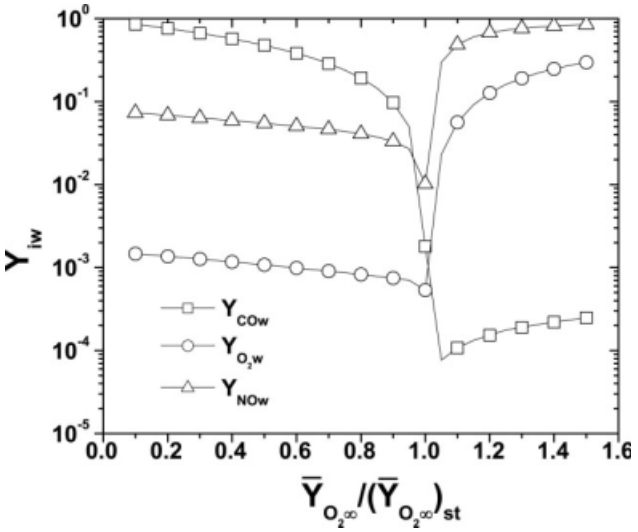

Figure 7. Minimum values of the reduced concentration of gaseous species close to the catalytic wall as a function of the concentration of the molecular oxygen in the gases.

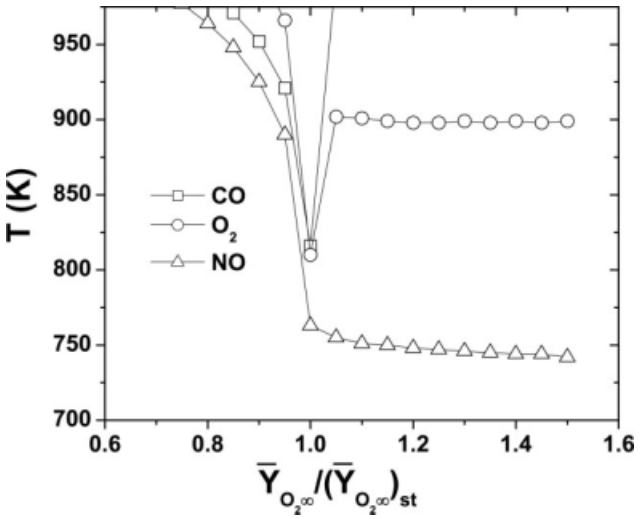

Figure 8. Temperature, where the minimum values of the reduced concentration of gaseous species close to the catalytic wall are obtained, as a function of the concentration of the molecular oxygen in the gases.

Figure 3 shows the values of parameters β and B_{O_2} as functions of temperature. The value of β increases drastically with temperature due to the activation energy of the desorption reaction of CO, while the mass number B_{O_2} decreases with temperature due to the assumed temperature dependence of the sticking probability of molecular oxygen and because of the square root of the collision term in the adsorption rate given in Eq. 11. This not negligible temperature dependence of the mass number, together with the temperature dependent $k_{1a\infty}$, must be considered in computing the ignition temperature given by Eq. 41, where a transcendental equation has to be easily solved. In the same figure, the parameter $2\beta\sqrt{B_{O_2}}$ is also plotted, which has to be unity at ignition. The resulting hysteresis behavior is shown in Figure 4, where the surface coverage of empty sites, θ_* is plotted as a function of β, where the middle unstable branch has not been resolved. The critical values of β at ignition and extinction are clearly shown. The response is similar to that obtained previously and shown in Figure 2.

Figure 5 shows the surface coverages of the adsorbed species as functions of the temperature, obtained with increasing temperature. At temperatures lower than that of ignition, the surface is mainly covered by adsorbed carbon monoxide molecules. As the ignition condition is reached, this species is replaced by empty sites, which makes the reaction to be very strong. All other coverages are found to be very small compared with unity. Thus, for all temperatures, the following is valid: $\theta_C \simeq 1 - \theta_*$. Figure 6 shows the reduced mass concentration for CO, NO, and O_2 as functions of temperature. At temperatures lower than ignition, all the three variables are close to unity, meaning no consumption at all. At ignition, all the three variables fall abruptly, reaching values of the order of 10^{-2}. As the temperature increases further, there is a slight decrease of the species reduced mass concentrations and after it all three increase with temperature.

To obtain the optimal concentration of molecular oxygen in the combustion gases, the removal efficiency of CO and NO is obtained for different values of the concentration of excess molecular oxygen in the gases. As shown in Figure 7, the minimum reduced mass concentration of all three species close to the wall are plotted as functions of the oxygen concentration related to that given by the overall stoichiometry, $\overline{Y}_{O_2\infty}/(\overline{Y}_{O_2\infty})_{st}$, where

$$(\overline{Y}_{O_2\infty})_{st} = \frac{1-\alpha}{2}\frac{W_{O_2}}{W_{CO}}\overline{Y}_{CO\infty}. \tag{46}$$

It is to be noticed that these minimum values are obtained at different temperatures. For rich gaseous mixtures, $\overline{Y}_{O_2\infty} < (\overline{Y}_{O_2\infty})_{st}$, carbon monoxide is not efficiently removed, whereas for lean mixtures, NO is not properly reduced. There is a narrow window close to stoichiometry where both pollutants are removed efficiently. Figure 8 shows the temperature where the maximum removal is produced as a function of the oxygen concentration. The temperature at stoichiometry is very close to the ignition temperature.

Conclusions

An analytical model based on numerical calculations of a simple catalytic pollutant remover was developed in this article. The dry combustion gases flowing in the stagnation-point flow geometry, contained carbon monoxide, nitrogen oxide, carbon dioxide, oxygen, and nitrogen. The optimal concentration of molecular oxygen was found to be dictated by the overall stoichiometry in the gases. The heterogeneous model used in this work considers a simple catalyst (in this cases platinum). To obtain an analytical solution, it was assumed that the concentration of nitrogen oxides, NO, is much lower than the corresponding of the carbon monoxide, CO, in the combustion gases, which is in general the case. For a high-removal efficiency, a large value of the mass transfer number B_{O_2} compared with unity is required, as in general this requisite is fulfilled. The solution is found be multivalued. The critical conditions of ignition (light-off) and extinction are obtained in closed form, in terms of the adsorption rates of molecular oxygen and carbon monoxide and the desorption rate of carbon monoxide. For simplicity, a stagnation-point flow configuration has been used. When using any other flow configuration, the results obtained in this work can be extracted by proper modeling of the characteristic length, l_f. The same is valid when using another catalyst, where the appropriate adsorption and desorption rates have to be used.

Acknowledgments

This work has been supported by DGAPA of UNAM, under contract IN113508. The support of CONACyT by grant PCI-033-13-07-07 is gratefully acknowledged.

Literature Cited

1. Koltsakis GC, Stamatelos AM. Catalytic automotive exhaust aftertreatment. *Prog Energy Combust Sci.* 1997;23:1–37.

2. Heck RH, Wei J, Katzer JR. Mathematical modeling of monolithic catalysts. *AIChE J*. 1976;22:477–484.
3. Baba N, Ohsawa K, Sugiura S. Analysis of transient thermal and conversion characteristics of catalytic converters during warm-up. *JSAE Rev*. 1996;17:273–279.
4. Oh SH, Cavendish JC. Transients of monolithic catalytic converters: response to step changes in feedstream temperature as related to controlling automobile emissions. *Ind Eng Chem Prod Res Dev*. 1982;21:29–37.
5. Montreuil CN, Williams SC, Adamczyk AA. Modeling current generation catalytic converters: laboratory experiments and kinetic parameter optimization-steady state kinetics. *SAE Paper*. 1992; 920096.
6. Pontikakis GN, Stamatelos AM. Identification of catalytic converter kinetic model using a genetic algorithm approach. *Proc Inst Mech Eng. Part D: J Automob Eng*. 2004;218:1455–1472.
7. Konstantinidis PA, Koltsakis GC, Stamatelos AM. The role of CAE in the design optimization of automotive exhaust aftertreatment systems. *Proc Inst Mech Eng. Part D: J Automob Eng*. 1998;212:169–186.
8. Deutschmann O, Schmidt R, Behrendt F, Warnatz J. Numerical modeling of catalytic ignition. In: *Twenty-Sixth Symposium (International) on Combustion*. Pittsburgh, PA: The Combustion Institute, 1996;27:1747.
9. Seo YS, Kang SK, Han MH, Baek YS. Development of a catalytic burner with pd/nio catalysts. *Catal Today*. 1999;47:421–427.
10. Treviño C. An asymptotic analysis of the catalytic ignition in a stagnation-point flow. *Combust Theory Model*. 1999;3:469–477.
11. Treviño C, Higuera FJ, Liñán A. Transient ignition and combustion of diluted hydrogen/air mixtures by a thin catalytic wire. *Proc Combust Inst*. 2003;29:981–988.
12. Rumminger MD, Hamlin RH, Dibble RW. Numerical analysis of a catalytic radiant burner: effect of catalyst on radiant efficiency and operability. *Catal Today*. 1999;47:253–262.
13. Treviño C, Prince JC. Catalytic combustion of dry carbon monoxide by external power activation. *Surf Sci*. 2000;449:61–74.
14. Treviño C, Prince JC, Tejero J. Catalytic ignition of dry carbon monoxide in a stagnation–point flow. *Combust Flame*. 2000;119:502–512.
15. Li Y, Armor JN. Catalytic reduction of nitrogen oxides with methane in the presence of excess oxygen. *Appl Catal B*. 1992;1:L31–L40.
16. Kikuchi E, Ogura M, Aratani N, Sugiura Y, Hiromoto S, Yogo K. Promotive effect of additives to in/h-zsm-5 catalyst for selective reduction of nitric oxide with methane in the presence of water vapor. *Catal Today*. 1996;27:35–40.
17. Amiridis M, Zhang T, Farrauto R. Selective catalytic reduction of nitric oxide by hydrocarbons. *Appl Catal*. 1996;10:203–227.
18. Mantri D, Aghalayam P. Detailed surface reaction mechanism for reduction of NO by CO. *Catal Today*. 2007;119:88–93.
19. Schlichting H, Kestin J. *Boundary-Layer Theory*,7th ed. New York: Springer Verlag, 2000.
20. Williams FA. Combustion Theory,2nd ed. Palo Alto, CA: Benjamin Cummings Publishing Co., 1985.
21. Harmsen J. Kinetic Modelling of the Dynamic Behaviour of an Automotive Three-Way Catalyst Under Cold-Start Conditions. Ph.D. thesis. Eindhoven, Netherlands: Eindhoven University of Technology, 2001.

Appendix

In this appendix, the special case of absence of molecular oxygen in the gases is considered, that is, the case with $\alpha = 1$. In this case, the oxygen needed for the reaction of the carbon monoxide comes from that delivered by the reduction of the nitrogen oxides. The concentration of NO needed to reach this condition is $Y_{NO_\infty} = Y_{CO_\infty} W_{NO}/W_{CO}$. In this limit, the reaction rate is not dictated by the adsorption of molecular oxygen and has to be obtained in a different way.

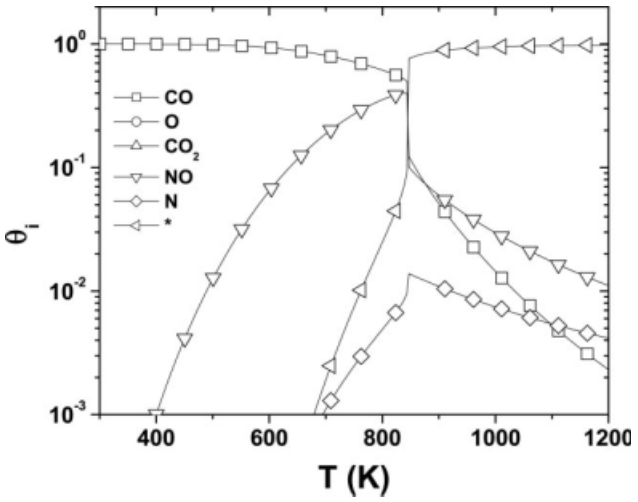

Figure A1. Surface coverage of adsorbed species as functions of the temperature, obtained as the temperature increases.

Because of the relatively high concentration of nitrogen oxides, the balance of the adsorbed species covering the catalyst includes besides θ_{CO} and θ_*, the contribution of θ_{NO}. That is,

$$\theta_{CO} + \theta_* + \theta_{NO} \simeq 1. \tag{A1}$$

Figure A1 shows the surface coverages obtained numerically for all adsorbed species as functions of the temperature. Except for θ_{CO}, θ_*, and θ_{NO}, the contribution of all other surface coverages are smaller than 10^{-2}. In this case, θ_{NO} now is of order unity, the light-off temperature is close to 850 K, with an hysteresis behavior as shown in Figure A2, for the surface coverage of empty sites as a function of temperature. Figure A3 shows the reduced concentration of pollutants close to the surface as functions of the temperature. At temperatures close to 844 K, the concentrations falls

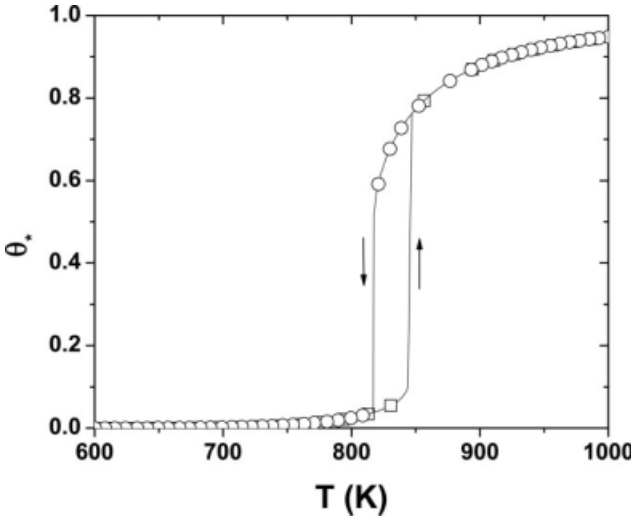

Figure A2. Surface coverage of empty sites, showing the hysteresis behavior.

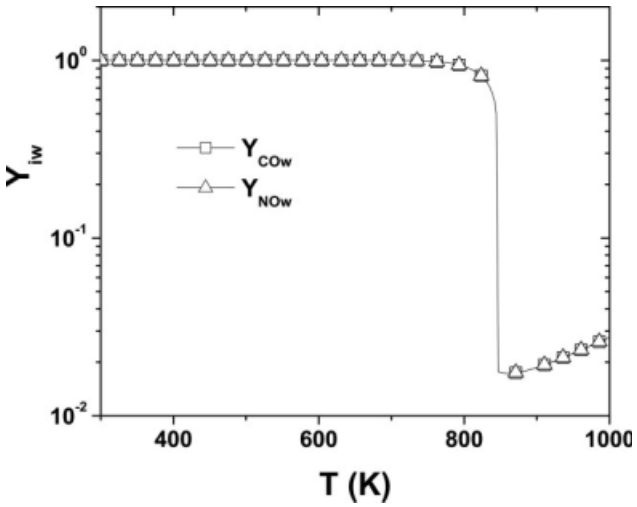

Figure A3. Reduced concentrations of CO and NO as functions of temperature.

down rapidly, reaching the minimum and increasing again with temperature. Also in this limit, the adsorption and desorption rates of both main species, CO and NO, are much more higher (several orders in magnitude) than the reaction rates, indicating that the surface coverages of the adsorbed species can be obtained from the Langmuir isotherms (partial equilibrium between adsorption and desorption). In this case, $\beta \sim \beta_5$ and $\theta_{NO} \simeq (\beta/\beta_5)\theta_{CO}$ from Eq. 35 is also of order unity. Using the balance Eq. A1, then

$$\theta_{CO} \simeq \frac{1-\theta_*}{1+\beta/\beta_5} \text{ and } \theta_{NO} \simeq \frac{1-\theta_*}{1+\beta_5/\beta}. \tag{A2}$$

The reaction rate is then

$$\omega_{NO} = \omega_{CO} = \Gamma k_7 \theta_{NO}\theta_* \simeq \frac{\Gamma k_7 \theta_*(1-\theta_*)}{1+\beta_5/\beta}. \tag{A3}$$

From Eqs. 13 and 28, the reduced mass concentration of CO close to the catalytic surface is

$$Y_{COw} = \frac{\widetilde{\beta}(1-\theta_*)}{\theta_*} = 1 - B_{CO}\theta_*(1-\theta_*), \tag{A4}$$

where $\tilde{\beta} = \beta(1+\beta/\beta_5)$, and B_{CO} is the mass transfer number given by

$$B_{CO} = \frac{\Gamma k_7 W_{CO} l_f I}{\mu_\infty \overline{Y}_{CO\infty}(1+\beta_5/\beta)}, \tag{A5}$$

appropriate for this limit, which strongly depends on temperature. Eq. A4 gives rise to a cubic equation for θ_* as a function of two parameters: $\widetilde{\beta}$ and B_{CO}, both of them strongly dependent on temperature. Assuming that the surface coverage of vacant sites is small compared with unity at ignition, that is, $1 - \theta_* \simeq 1$, Eq. A4 can be reduced to a quadratic equation given by

$$\widetilde{\beta} = \theta_* - B_{CO}\theta_*^2,$$

with solution

$$\theta_* = \frac{1 \pm \sqrt{1 - 4B_{CO}\widetilde{\beta}}}{2B_{CO}}. \tag{A6}$$

Ignition occurs when $B_{CO}\widetilde{\beta} = 1/4$. The ignition temperature can be obtained after solving this transcendental equation.

Manuscript received Mar. 23, 2009, and revision received May 26, 2009.